

A New Boundary-Based Shape Recognition Technique

I. Tchoukanov

R. Safaei-Rad

B. Benhabib

K.C. Smith

Computer Integrated Manufacturing Laboratory, Department of Mechanical Engineering
University of Toronto, 5 King's College Road, Toronto, Ontario, M5S 1A4, CANADA

ABSTRACT - In this paper, a new 2D-Shape-encoding scheme is introduced which is based on the idea of the Angle-Of-Sight (AOS). Using this scheme, a shape can be efficiently transformed into a 1D signature by recording the AOS-vs-distance of each boundary point with respect to a shape-specific Chord-Of-Sight (COS). The COS is selected by using an extension of the notion of shape boundary, to the idea of shape-specific points and the characteristic ellipse (CE). The AOS signature has many important properties including: It is information-preserving, and thus unique; It does not require boundary smoothing; It has its own selectable smoothing property; It can provide a set of multi-scale representations by means of a simple operation; It is transformation-invariant; It is defined at all points; It preserves symmetries. As well, for matching purposes, a two-level matching process is proposed using a global measure (the eccentricity of the CE of a shape) and a dissimilarity measure based on the AOS signature. The encoding and matching techniques developed have been tested with 35 manufactured objects. The results obtained show that the AOS signature and the two-level-matching technique are quite effective and reliable for the recognition of 2D-shapes of typical manufactured objects.

1. Introduction

Shape representation and matching is a key problem in machine-vision-system development. This problem arises, as well, in the context of a new active-vision system for 3D-object-recognition in robotic assembly workcells, under development in the Computer Integrated Manufacturing Laboratory (at the University of Toronto) [1-2]. In the latter development, the main design concept is to reduce the dimensionality of the recognition task: A 3D object is modeled in this system by using a small set of topologically distinct perspective views, called *standard-views*. The process of shape matching is performed between the acquired 2D standard-view of the sensed object with unknown identity and a library of 2D standard-views of a set of objects. Consequently, any usable 2D representation and its corresponding recognition technique must be *position-, rotation-, and scale-invariant*.

Here, following the same concept of dimensionality reduction in a "top-down" fashion, the problem of the design of a transformation-invariant 2D-shape-encoding scheme is addressed. Our goal has been the identification of a methodology by which the 2D standard-views are transformed into 1D signatures suitable for signal matching. Here the required

signature is defined as a 1D signal derived from the shape by using an encoding scheme for mapping the information from the 2D "shape" space to the 1D "signature" space.

The new 2D-shape-encoding scheme is based on a new concept, *the angle-of-sight*, for extracting and encoding "shape" information [3], and has the following properties: It is easily computed from a chain code and thus has a low processing/memory requirement; It is information-preserving and thus unique; It does not require boundary smoothing since it is not based on first or second derivatives of the boundary; It has its own inherent smoothing property; It can provide a set of multi-scale representations by means of a simple operation; It is position-invariant, rotation-invariant (through standardization of a starting point), and size-invariant (through a simple normalization of the perimeter length -- the signature is required to be normalized only along *one* axis); It is a single-valued function, defined at all points, and does not have abrupt changes in the signature amplitude; The shape of each object is encoded by only one function (the signature) as opposed to two (as in the rectangular representation); It preserves symmetries; It represents deviation from a basic shape (the circle), and as a result, it can be used for creating a measure to test circularity; and, It is a stable representation in the sense that small changes in the boundary will have an adequately small effect on the signature.

In Section 2, the new 2D shape-encoding scheme, which is based on the idea of the angle-of-sight (AOS), is introduced. In Section 3, the properties of the new AOS signature are discussed. Matching of AOS signatures is addressed in Section 4. Experimental results are presented and analyzed in Section 5. A brief summary is given in Section 6.

For the complete report on the proposed technique, please refer to [4].

2. The Proposed Boundary-Based 2D-Shape Representation Technique

In this paper, a "shape" is defined as a simply connected compact region in a two-dimensional Euclidean space, which may or may not be convex [5]. The set of boundary or frontier points of this region are used to characterize its shape.

2.1. Description of the Angle-of-Sight Shape-Representation Scheme

The angles of a triangle formed by any three non-collinear boundary points *C, D* and *E* of a 2D shape (Figure 1) are invariant under shape translation, rotation and scaling. The

following thought experiment can be performed to visualize the use of this property in a shape-encoding scheme: *Predetermine* two of the vertices, say C and D , and keep them fixed while moving the third vertex E along the shape's boundary (Figure 1). The angle α , associated with each position of the moving vertex E , is a descriptive property of the boundary and can be used for shape representation. Hereafter, the chord joining the fixed points is referred to as the chord-of-sight (COS) and the angle α formed at the third vertex is referred to as the angle-of-sight (AOS).

The AOS signature is a boundary-based descriptor of a planar shape and defined as a 1D signal $AOS = \alpha(l)$, where l is the arc length between a starting point E_0 and the boundary-tracing point E in the clockwise (or counterclockwise) direction:

$$\alpha(l) = \arccos \left[\frac{d_1^2(l) + d_2^2(l) - d^2}{2d_1(l) d_2(l)} \right], \quad \alpha(l) \subseteq (0, \pi) \quad (1)$$

where $d_1(l)$ and $d_2(l)$ are the distances from the tracing point to the end-points of the COS, and d is the length of the COS.

The AOS signature of a planar shape with *normalized boundary length* is translation- and scale-invariant. It is a periodic signal, and thus, a change of the starting-point position causes only a cyclic shift of the signature.

In order to make the signature rotation-invariant as well, its starting point must be standardized. In that respect, the AOS encoding scheme uniquely defines an orthogonal shape-specific coordinate system, which can be used to select a "standard" starting point E_0 . The geometry of this situation can be studied using Figure 2. The loci of boundary points having one and the same AOS are circular arcs passing through the end-points of the COS. The locus of the centers of these constant AOS arcs is a straight line orthogonal to the COS and passing through its midpoint. The intersection points of this line and the boundary are object-specific points, and each can be used as the starting point for the AOS signature. To make the starting point unique, the most distant (or the least distant) intersection point to the origin of the shape-specific coordinate system (point O in Figure 2) can be used. If there is more than one such point (typically a rare case for industrial shapes), then a like number of shifted signatures must be derived. Subsequent to standardization of the starting point E_0 , the AOS signature becomes rotation-invariant as well.

2.2. Chord-of-Sight Selection Requirements

The AOS encoding scheme implies that the positions of the COS end-points are *predetermined* by an off-line selection process, whereas their locations are detected in real time. Obviously, the AOS signature of a shape is transformation-invariant only if one and the same pair of COS end-points is unambiguously detected for each position, orientation, and size of the shape. As far as the shape-recognition problem is concerned, matching AOS signatures is to be performed only

if they are derived with reference to a COS with one and the same identity. Therefore, COS-selection requirements must be established. The COS end-points must have the following properties:

- *Uniqueness*: The COS end-points must be uniquely identifiable from the shape boundary (or features derived from it);
- *Commonality*: The COS end-point determination must rely on features common to a given set of shapes;
- *Boundary-distortion tolerance*: The COS end-points must be chosen so as to be minimally sensitive to boundary noise; and,
- *Detectability*: The COS end-points must be identified fast and readily.

The last requirement is in contradiction with the first three. The first three can be satisfied by points having a large domain of support. However, as a consequence, detection of such prominent points (in a pointwise sense) would require considerable computational time. Points relying on a local domain of support, such as corners, dominant points, etc., can hardly meet the above-stated requirements. Generally, the end points of the longest boundary primitives, such as linear or curved segments, are better candidates for the COS end-points, but their detection requires considerable processing time [6-7].

Ideally, the best candidates for the COS end-points are points to whose coordinates all boundary points collectively contribute.

2.3. Chord-of-Sight Based on Shape-Specific Points

The concept of shape-specific points is an extension of the notion of shape to include points which do not lie on the shape boundary. The formal definition of a shape-specific point is given in [8], and for the sake of clarity, it will be repeated here:

"Let $p = F(S)$ be a point computed from shape S according to procedure F . Also, let $S' = T(S)$, where T is a planar transformation (translation, rotation, or dilation), and let $p' = F(S')$. Then p is a shape-specific point of S with respect to transformation T if and only if $p' = T(p)$."

This definition also applies to geometrical entities other than points. For instance, the length of a chord connecting two shape-specific points is shape-specific as well.

Shape-specific points have several properties which make them attractive to the AOS encoding scheme:

- Shape-specific points behave as if they were on the shape boundary;
- The coordinates of shape-specific points are computed rather than detected; and,
- All boundary points collectively contribute to the computation of the coordinates of shape-specific points. In this

sense, the whole shape's boundary acts as a domain of support for each shape-specific point.

An AOS signature derived with respect to a COS, which is based on shape-specific points, retains the property of being shape-transformation-invariant. The method for selection of the starting point of a signature, presented in Section 2.1, is applicable to shape-specific COS end-points as well.

Various functions can be defined for shape-specific-point computation. Mitiche and Aggarwal in their work [8] employed the centroid and the weighted median point to recover shape orientation for the purpose of registration. However, simulated experiments here have indicated that boundary noise causes a significant shift in the starting point position of the corresponding AOS signature when these two points are used to define the COS.

In view of the above consideration, better results can be achieved by using shape-specific points which are computed from a Fourier expansion of the rectangular representation of a shape. Kuhl and Giardina [9] have applied a Fourier trigonometric expansion to the X and Y projections of a closed contour and have shown that the locus of each vector of constant frequency is elliptical. The five basic parameters of the ellipse related to the fundamental Fourier harmonic are given in [10]. It has been proven that this ellipse is shape-specific [2]. Thus, it can be said that this shape-specific ellipse is an important extension of the notion of shape. Hereafter, the shape-specific ellipse related to the first harmonic (the fundamental frequency) will be referred to as the Characteristic Ellipse (CE). As an example, the AOS signature of a triangle is shown in Figure 3. The crossing points of the shape boundary and the major axis of the CE are used as the COS end-points.

2.4. An Improved 3D-Based AOS Encoding Scheme

The AOS function is not defined for boundary points which are collinear with the end-points of the chord-of-sight, and therefore, the associated signature suffers from having jump discontinuities for such points. Jump discontinuities hinder matching of signatures and deteriorate the spectral characteristics of the signal (through Gibb's phenomenon). This is a common drawback of many boundary-based encoding schemes [11].

This problem can be solved by placing one of the end-points of the COS outside of the plane of the shape. An orthogonal XYZ frame is considered herein to achieve this (Figure 4), where the origin coincides with the center of the characteristic ellipse of the boundary, and the X and Y axes are aligned with its major and minor radii. The length of the COS is defined to be equal to the major (or minor) radius of the characteristic ellipse of the boundary. In the same manner as in Section 2.1, the AOS signature is defined as a 1D signal $AOS = \alpha(l)$, where l is the arc length between the moving point E and a starting point E_0 , measured in a clockwise (or counterclockwise) direction. Note that, as a result of employ-

ing the third dimension, the AOS function has no discontinuities. Based on this new definition of COS, the AOS function is defined as follows:

$$\alpha(l) = \arctan \left[\frac{A}{r(l)} \right], \quad \alpha(l) \subseteq (0, \pi/2), \quad (2)$$

where A is the length of the major radius of the characteristic ellipse of the boundary (the minor radius B of CE can be used as well), and $r(l)$ is the distance from a boundary point to the origin of XYZ frame. The crossing point of the boundary and the Y -axis or X -axis (which are respectively aligned with the major and minor axes of the characteristic ellipse of the shape), which is the most distant (or least distant) from the origin of the XYZ frame, can be used as a "standard position" for the starting point.

Figure 5 shows a set of simulated shapes and their AOS signatures as proposed in this section.

3. The Properties of the AOS Signature

The improved version of the AOS encoding scheme has the following important properties:

- It can easily be computed from a chain code and has a low processing/memory requirement.
- The signature preserves shape symmetry in the sense that points equidistant from the origin of the XYZ frame have equal angles-of-sight.
- It is inherently position-invariant, and, through standardization of the starting point, it is easily made rotation-invariant. Furthermore, by normalizing the boundary length of a shape, the signature becomes size-invariant as well.
- The signature is a single-valued function, defined at all points, and does not yield abrupt changes in the signature amplitude due to its inherent smoothing property.
- The simplest possible signature (a straight line) belongs to the circle -- the basic shape. In this sense, the AOS signature shows how a shape deviates from the basic shape. This property can be used to define a new measure-for-circularity test.
- The problem of oversampling/undersampling of the boundary for the AOS signature is significantly less severe than similar encoding techniques such as polar representation, since the signature is based on contour *sequence* (the Freeman chain code).
- It is a stable representation, since small changes in the boundary will have small effects on the signature (thus it is stable under noise such as that from quantization). A reason for this is the inherent smoothing property of the proposed encoding scheme.
- It provides an inherent smoothing of the shape representation, since the amplitude of the transfer function $y = \arctan(x)$ is always under the line $y = x$. Also, the signature can easily be further smoothed by increasing the length of the

COS. This latter property can be employed selectively for boundary-noise reduction. Longer COS's cause smoothing of the form of the signal and an increase of its DC component. Thus, due to the smoothing property of the AOS encoding scheme, a multiscale shape representation can be generated without pre-processing of the shape boundary.

- The AOS signature preserves shape information to the effect that the original shape can be uniquely recovered from the signature. More details concerning this property of the AOS signature is given in [4]. By the virtue of this property, the AOS signature is appropriate for data compression and shape recognition.

4. Matching of AOS Signatures

As shown in [2], the characteristic ellipse (CE) of any planar shape is a shape-specific ellipse, which thus behaves as an inseparable part of the shape. Conceptually, it can be said that each shape is "accompanied" by such a characteristic ellipse. This idea suggests that two shapes can be matched by first aligning their characteristic ellipses. This process of alignment in the image plane can be performed in two steps: First, superimpose the two shapes so that their CE centers coincide, and subsequently, rotate one of the shapes until the major/minor axes of their characteristic ellipses align. Alignment of shapes in the image plane is equivalent to superimposing their AOS signatures, recalling that the AOS signature is transformation-invariant, and that its starting point lies on the major axis (or minor axis) of the characteristic ellipse.

Conceptually, if two shapes are similar, a dissimilarity measure of their signatures is expected to achieve its global minimum within a small 1D window, ∇ , centered around the starting point of the superimposed signatures. This windowed "shift-and-match" search is necessary to allow for possible *noise-induced* displacement of the characteristic ellipse (due to the variabilities in boundary quantization, edge detection, and shape orientation). It is proposed to use the following average pointwise dissimilarity measure:

$$D(j) = \frac{1}{K} \sum_{i=0}^{K-1} \left[S_1(i) - S_2(i+j) \right]^2, \quad j \in [-\nabla, \nabla], \quad (3)$$

where $S_1(i)$, $i=0,1, \dots, M-1$, and $S_2(i)$, $i=0,1, \dots, N-1$, are two shape signatures (two discrete ordered sequences), M and N are the total numbers of elements in the ordered sequences (for example, the total number of links in Freeman chain code), and $K = \min(M, N)$.

If the eccentricity of the CE is above a certain threshold, the shape can be considered rotationally symmetrical. For such shapes, the starting point, as defined in Section 2.1, is not unique. Thus, the axes of the CE cannot be used for superimposition of shapes. In [12], Freeman proposes using min-max points of a curvature-based signature for starting-point selection. This idea can be extended and implemented for alignment of min-max points of the AOS signatures to achieve proper superimposition of the shapes to be matched.

Evidently, if two shapes are similar, there is a correspondence between the min-max points of their signatures, and the dissimilarity measure is minimized by proper alignment of min-max points. One should notice that the geometrical interpretation of the min-max points of an AOS signature is as follows: a maximum extremum point corresponds to a concavity of a shape or is caused by a long linear segment, while a minimum extremum point corresponds to a corner (a vertex). In this sense, alignment of AOS signatures by using pairs of maximum (or minimum) extremum points can be considered as superimposition of edges (or vertices) of the shapes to be matched. For more details on edge-based shape alignment, the reader can refer to [13]. Shape matching through alignment of features like edges or vertices implies searching for those pairings of maximum (or minimum) extremum points whose alignment would minimize the dissimilarity measure. To avoid considering all possible combinations, we confine the search process only to the min-max points which are dominant, i.e., having a high (or the highest) domain of support. Correspondingly, we have implemented the algorithm presented in [14] for detection of extremum points of the AOS signatures, and for ordering them in accord to their domain of support.

5. Experimental Procedure and Results

In order to test the proposed encoding and matching schemes, 35 randomly-selected manufactured objects were considered (some of them are shown in Figure 6). The range of their sizes (in terms of area and perimeter length) is quite large; They represent simple and basic as well as very complex shapes; as well, the eccentricity values of their CE's are well-distributed.

To generate the set of reference shapes for the set of objects, the following procedure was employed:

- The objects were positioned in the scene such that the major axes of their CE's would be almost horizontal, and, as well, they would be at the center of the field of view of the camera. This position is referred to as the standard reference position;
- The camera was located directly over each object and its focal length and aperture size were adjusted for each object;
- A backlit-illumination system was employed so that the silhouette of the object can be acquired;
- The boundary of the silhouette was obtained by applying binary thresholding and edge-tracing techniques.

The set of test shapes, on the other hand, was generated with procedures similar to those above, but with the following differences:

- The objects were randomly positioned and oriented;
- The focal length and aperture size of the camera were fixed (at average values) for all the test objects.

Subsequent to the generation of AOS signatures (both the reference and test ones), the proposed matching technique was applied. In this regard, the following aspects of the process must be noted:

- The size of the 1D window for the "shift-and-match" search process was assumed to be 1/20 of the perimeter length of a shape. This is, generally, a relatively large window compared to the actual required size for many test shapes. However, it was accepted in order to provide a higher degree of confidence in the results obtained. Furthermore, the size of the window can be *objectively* predetermined according to some measure which is a function of perimeter length, complexity-measure value, and eccentricity of the CE's of a set of shapes.
- In case of rotationally-asymmetric shapes, since the matching procedure is based on the alignment of the major and minor axes of CE's of two shapes, there exists a π -ambiguity in the alignment process. This must also be taken into account in the matching algorithm.
- To determine the presence of centrally symmetric shapes, the value 0.95 was used as an eccentricity threshold. This value was determined experimentally. In the set of 35 shapes under consideration, four of them are classified as centrally symmetric (shapes number 18, 26, 27, and 32).
- The size of the COS for each shape was selected to be the mean value of its CE's major and minor radii.

Based on the above considerations, each *test* signature was compared with the 35 *reference* signatures. In order to reduce the search space, a two-level matching process was employed: in the first level, a global measure is used to reduce the search space; in the second level, the AOS signature of the test shape is compared, through a dissimilarity measure, with the set of AOS reference signatures in the reduced search space. The eccentricity of the characteristic ellipse (CE) of each shape (which is defined as the ratio of minor and major radii) was used as a *global* scalar measure.

The results of the experiment on all 35 *test* shapes (signatures) are shown in Table 1. As can be seen from this table, 33 of the 35 test shapes are classified correctly. Amongst this group, 3 are classified correctly but with a low degree of confidence; that is, in 3 cases there exists a *next* closest candidate whose dissimilarity distance value is less than twice that of the first candidate (see the notes associated with Table 1). On the other hand, there are 2 test shapes that are misclassified through the minimum distance rule: numbers 25 and 27. In these instances, the dissimilarity caused by quantization error predominates over the geometric dissimilarity, which results in misclassification. This is due to the fact that the corresponding dissimilarity measure values are small and quite close to each other.

Based on the experimental results, it can be said that the matching scheme leads to a high degree of correct classi-

fication.

6. Summary

In this paper, we addressed the problem of designing a new transformation-invariant 2D-shape-encoding scheme, by which 2D standard-views were transformed into 1D signatures suitable for signal matching. In this context, the following aspects of the proposed technique were discussed: the 3D-based AOS encoding scheme, the characteristic ellipse of a 2D shape and its shape-specific property, the properties of the AOS signature, a matching scheme for AOS signatures based on a dissimilarity measure, and the eccentricity of the CE of a shape as a global measure for reduction of search space. In order to test the proposed encoding and matching techniques, 35 manufactured objects were considered. The results obtained show that the AOS signature encoding scheme and the two-level matching technique are quite effective and reliable in the process of recognition of manufactured objects.

References

- [1] Safaee-Rad, R., Benhabib, B., Smith, K.C., and Zhou, Z., "Pre-Marking Methods for 3D Object Recognition", *IEEE, Proc., Int. Conference on Systems, Man, and Cybernetics*, Cambridge, MA, Vol. II, pp. 592-595, Nov. 1989.
- [2] Safaee-Rad, R., "An Active-Vision System for 3D-Object Recognition in Robotic Assembly Workcells", *Ph.D. dissertation*, University of Toronto, Toronto, ON, Sept. 1991.
- [3] Tchoukanov, I., Safaee-Rad, R., Benhabib, B., and Smith, K.C., "The Angle-of-Sight Signature for 2D Shape Analysis", *IEEE, Proc., Int. Conference on Acoustics, Speech, and Signal Processing*, Toronto, ON, Vol. 4, pp. 2461-2464, May 14-17, 1991.
- [4] Tchoukanov, I., Safaee-Rad, R., Smith, K.C., and Benhabib, B., "The Angle-of-Sight Signature for 2D Shape Analysis of Manufactured Objects", *Pattern Recognition*. (To appear)
- [5] Smith, S.P., and Jain, A.K., "Chord Distribution for Shape Matching", *Computer Graphics and Image Processing*, Vol. 20, pp. 259-265, December 1982.
- [6] Ballard, D.H., "Generalizing the Hough Transform to Detect Arbitrary Shapes", *Pattern Recognition*, Vol. 13, No. 2, pp. 111-122, 1981.
- [7] Liao, Y., "A Two-Stage Method for Fitting Conic Arcs and Straight-Line Segments to Digitized Contours", *IEEE, Proc., Int. Conference on Pattern Recognition and Image Processing*, pp. 224-229, 1981.
- [8] Mitche, A., and Aggarwal, J.K., "Contour Registration and Shape-Specific Points for Shape Matching", *Computer Vision, Graphics, and Image Processing*, Vol. 22, pp. 396-408, 1983.
- [9] Kuhl, F.P., and Giardina, C.R., "Elliptical Fourier Features of a Closed Contour", *Computer Graphics and Image Processing*, Vol. 18, pp. 236-258, 1982.
- [10] Safaee-Rad, R., Smith, K.C., Benhabib, B., and Tchoukanov, I., "Application of Moment and Fourier Descriptors to the Accurate Estimation of Elliptical Shape Parameters", *IEEE, Proc., Int. Conference on Acoustics, Speech, and Signal Processing*, Toronto, ON, Vol. 4, pp. 2465-2468, May 1991.
- [11] Marshall, S., "Review of Shape Coding Techniques", *Image and Vision Computing*, Vol. 7, no. 4, pp. 281-294, November 1989.
- [12] Freeman, H., "Use of Incremental Curvature for Describing and Analyzing Two-Dimensional Shape", *IEEE, Proc., Computer Society Conference on Pattern Recognition and Image Processing*, Chicago, Illinois, pp. 437-444, Aug. 1979.
- [13] Kashyap, R.L., and Oomen, B.J., "A Geometrical Approach to Polygonal Dissimilarity and Shape Matching", *IEEE Trans. on Pattern*

[14] Teh, Cho-Huak, and Chin, R.T., "A Scale-Independent Dominant Point Detection Algorithm", Proc., Int. Conference on Computer Vision and Pattern Recognition, pp. 229-234, June 1988.

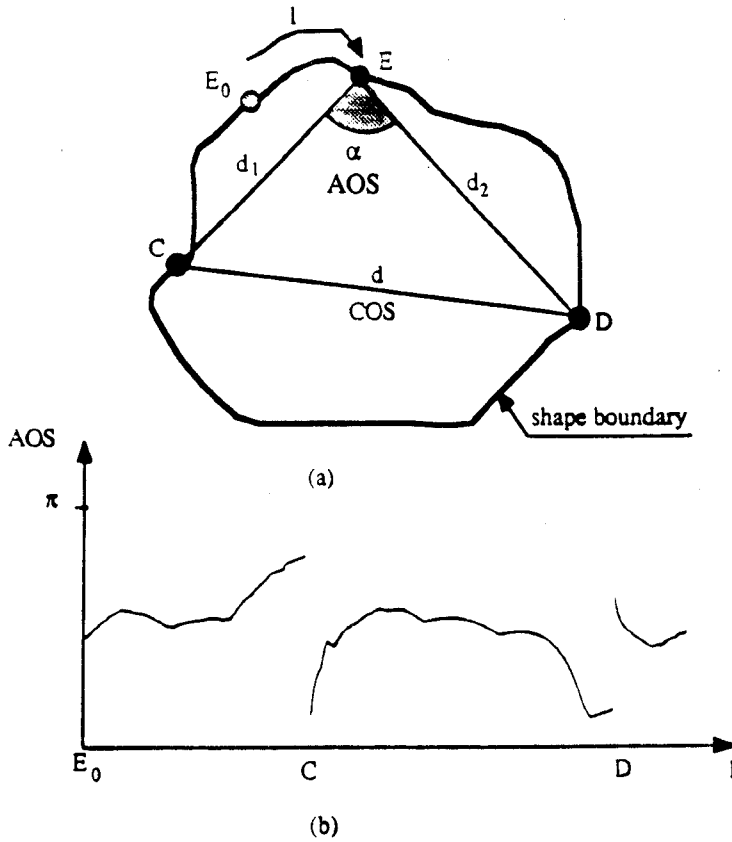


Figure 1(a) Definition of the angle-of-sight. (b) The derived signature.

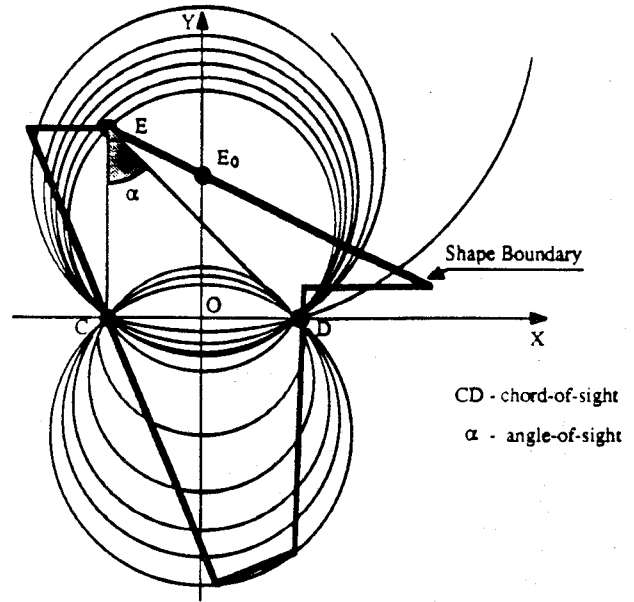


Figure 2. The AOS-related coordinate system.

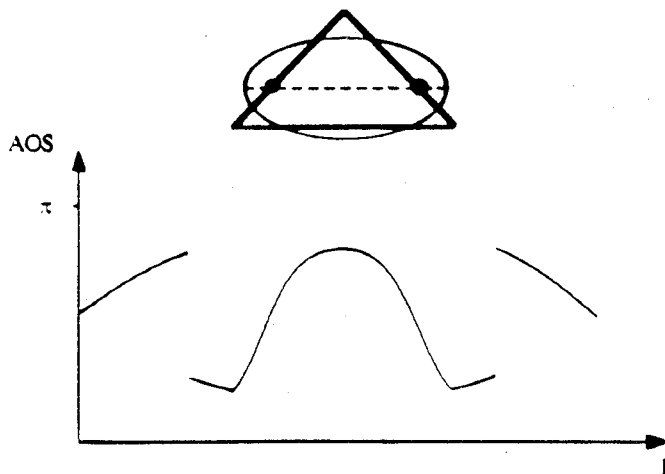


Figure 3 The AOS signature of a triangle.

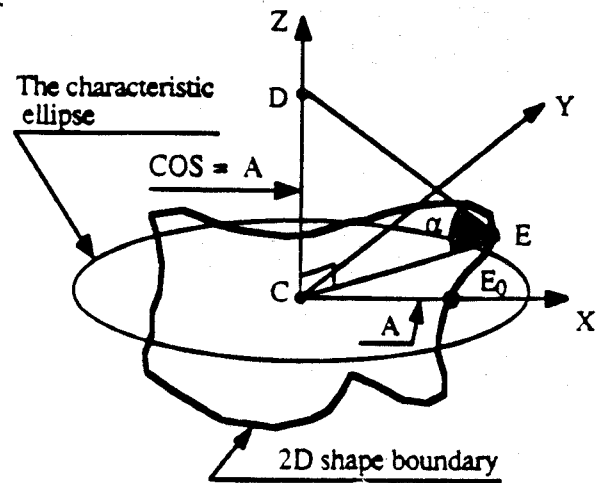


Figure 4 Definition of an improved angle-of-sight scheme.

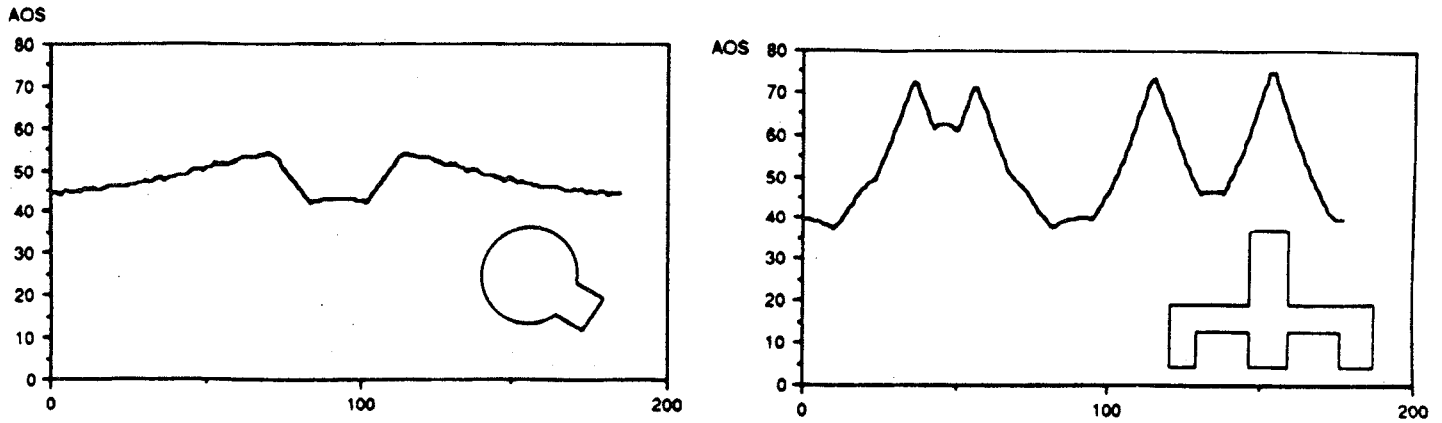


Figure 5. AOS signatures of a set of simulated shapes.

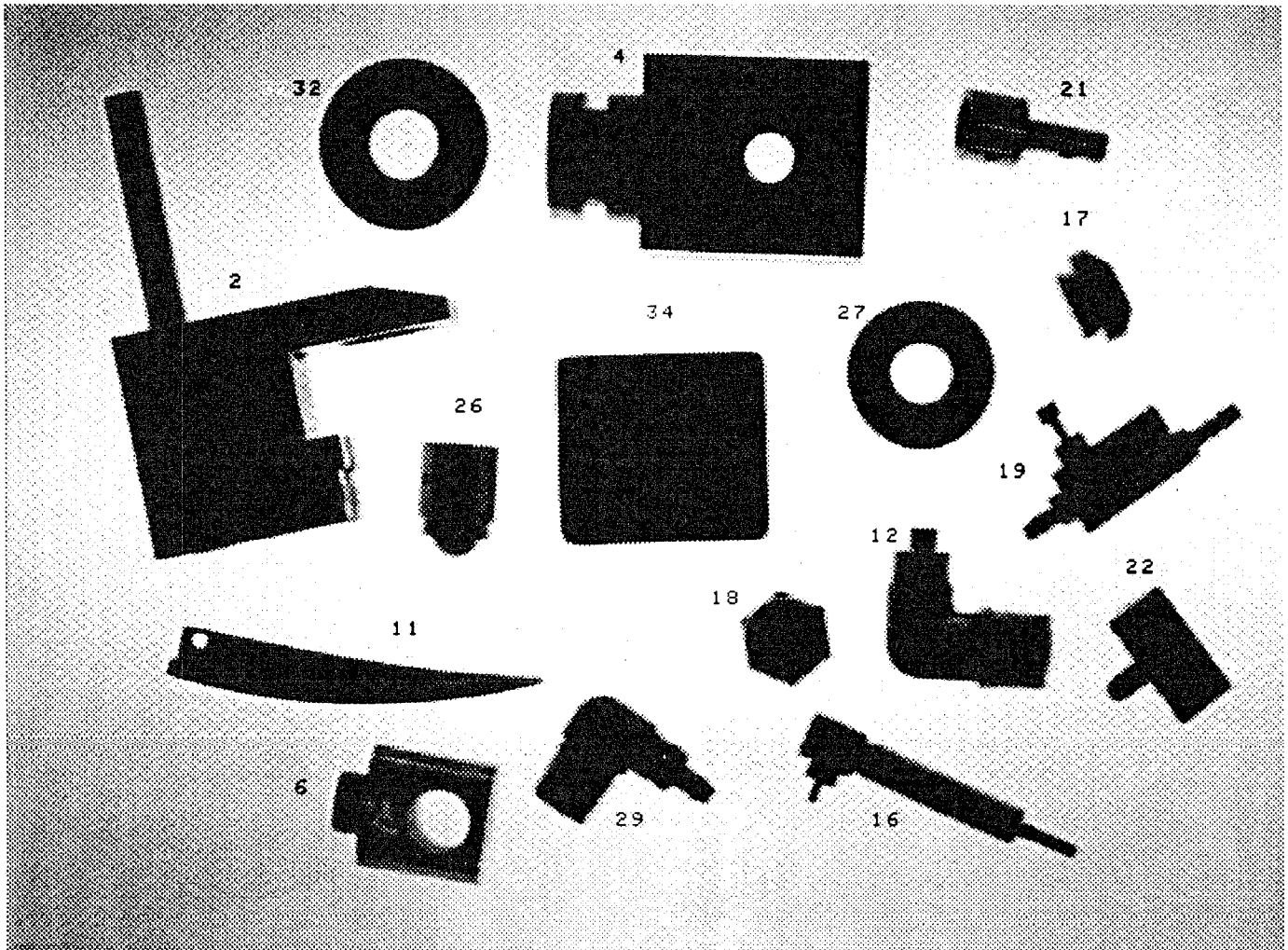


Figure 6. A back-lit image of manufactured objects used in the experiment

Test Shape	Closest Candidate		Next Closest Candidate		Correctly Classified		Mis-classified	RNCBEM #
	No.	MDV*	No.	MDV	LMDV	MMDV		
# 01	# 01	0.876	# 16	12.644	√			8
# 02	# 02	0.194	# 29	93.875	√			3
# 03	# 03	0.165	# 35	5.688	√			3
# 04	# 04	0.778	# 26	9.136	√			3
# 05	# 05	0.006	# 25	0.698	√			7
# 06	# 06	0.134	# 26	4.063	√			4
# 07	# 07	1.107	# 23	135.314	√			2
# 08	# 08	0.749	# 19	76.013	√			4
# 09	# 09	0.735	# 13	0.990		√		3
# 10	# 10	0.076	# 09	1.269	√			4
# 11	# 11	0.194	# 31	8.969	√			7
# 12	# 12	0.351	# 30	8.024	√			3
# 13	# 13	0.055	# 14	1.658	√			4
# 14	# 14	0.054	# 13	2.435	√			3
# 15	# 15	0.142	# 05	0.998	√			8
# 16	# 16	0.177	# 25	7.485	√			8
# 17	# 17	0.408	# 23	7.556	√			3
# 18	# 18	0.165	# 32	1.5579	√			4
# 19	# 19	0.147	# 17	51.032	√			2
# 20	# 20	0.224	# 31	1.009	√			7
# 21	# 21	0.400	# 24	15.725	√			3
# 22	# 22	0.287	# 23	35.539	√			4
# 23	# 23	0.380	# 26	7.580	√			3
# 24	# 24	2.406	# 31	3.516		√		2
			# 20	4.275				
			# 14	4.355				
# 25	# 05	0.603	# 25	0.702			√	8
			# 15	0.806				
# 26	# 26	0.263	# 32	15.744	√			4
# 27	# 32	0.128	# 27	0.143			√	4
# 28	# 28	0.100	# 34	5.835	√			4
# 29	# 29	0.395	# 12	12.262	√			6
# 30	# 30	0.614	# 12	7.882	√			6
# 31	# 31	0.022	# 20	1.088	√			6
# 32	# 32	0.049	# 27	0.110	√			4
# 33	# 33	4.679	# 35	5.117		√		3
			# 05	7.627				
			# 25	7.824				
# 34	# 34	0.126	# 28	7.000	√			2
# 35	# 35	0.045	# 05	3.290	√			3

Notes: $COS = (A+B) / 2$; 1D Search Window Size = (Perimeter Length) / 20.
MDV*: The Smallest Mean-Distance Value
MDV: The Range of Mean-Distance Values of the Closest Candidates:
MVD* < MDV < 2 (MVD*)
LMDV: Large Mean Distance Value: LMDV > 2 (MDV*)
MMDV: Marginal Mean Distance Value: MVD* < MMDV < 2 (MDV*)
RNCBCM: Reduced Number of Candidates Based on Eccentricity Measure:
 $E_t - 0.05 < E < E_t + 0.05$

Table 1. Results of shape matching experiments.